CYBERNETICS AND PHYSICS, VOL. 9, NO. 1, 2020, 31–40

SELF-ORGANIZATION IN NETWORK MOTIFS OF THREE BISTABLE DUFFING OSCILLATORS

R. Jaimes-Reátegui, J. M. Castillo-Cruz, J. H. García-López
G. Huerta-Cuellar, L. A. Gallegos-Infante
Centro Universitario de Los Lagos
Universidad de Guadalajara
México
{rider.jaimes, harrisoncha744, jhgarcial, ghuertacuellar, gallegosarmando}@gmail.com

A. N. Pisarchik
Center for Biomedical Technology
Technical University of Madrid
Spain
Innopolis University, Russia
alexander.pisarchik@ctb.upm.es

Article history:
Received 17.11.2019, Accepted 17.06.2020

Abstract

We study the emergence of synchronization in the network motif of three bistable Duffing oscillators coupled in all possible configurations. The equation of motion is derived for every configuration. For each motif, we vary initial conditions of every oscillator and calculate the bifurcation diagram as a function of the coupling strength. We find transitions of the whole system to a monostable regime with either a fixed point or a limit cycle depending on the motif's configuration, as the coupling strength is increased. The most complex dynamics is observed the unidirectional chain, where a transition to quasiperiodicity occurs.

Key words

Bistability, bifurcation, coupled oscillators, network motif.

1 Introduction

Complex networks have been taking a prominent role in many aspects of modern science and society. It is widely accepted that large-scale dynamical properties of a network are governed by its much smaller constituent elements referred to as *network motifs* [Alon, 2007; Stone et al., 2019]. In technical terms, Milo et al. [Milo et al., 2002] defined motifs as "patterns of interconnections (or subgraphs) occurring in complex networks at numbers significantly higher than those in randomized networks". Their presence indicates the operation of underlying nonrandom structural or evolutionary design principles that might have been involved in building the network. In this respect, the knowledge of dynamics and synchronization of network motifs can help us in understanding self-organization of large networks [Boccaletti et al., 2006].

Synchronization and control of dynamical systems were studied by many researchers (for comprehansive review see [Andrievskii and Fradkov, 2004; Boccaletti et al., 2018]). Significantly less attention was paid to synchronization in network motifs of coupled oscillators. In this respect, it is worth mentioning interesting studies with Rössler [Kapitaniak et al., 2015], Rulkov [Sausedo-Solorio and Pisarchik, 2017; Pisarchik et al., 2019], Stuart-Landau [Karakaya et al., 2019], Hodgkin-Huxley [Mirasso et al., 2017], and other models [Suresh et al., 2016]. Concerning Duffing oscillators, we have to mention the paper of Jaros et al. [Jaros et al., 2016], who observed different bifurcation scenarios with respect to the coupling strength in three unidirectionally coupled Duffing oscillators.

In this paper, we study dynamics of simplest network motifs formed by three Duffing oscillators. The Duffing equation was introduced by German electrical engineer Georg Duffing [Duffing, 1918] to describe forced vibrations of industrial machinery. This prototypical dynamical system was then successfully explored to simulate various physical processes, such as stiffening

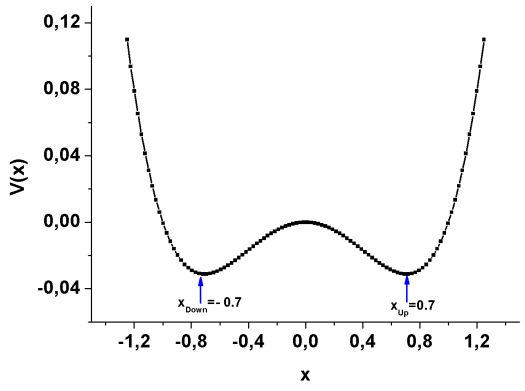

Figure 1. Double-well potential Eq. (2) for $a = -0.25$ and $b = 0.5$ with minima at $x_{\mathbf{D}own} = -0.7071$ and $x_{\mathbf{U}p} = 0.7071$ and a local maximum at $x = 0$.

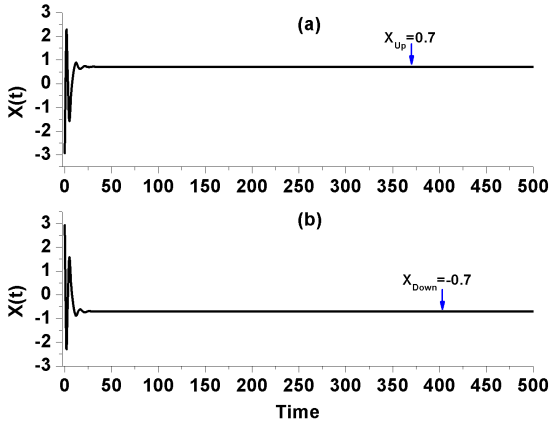

Figure 2. Time series of Eq. (1) for $\gamma = 0.4$, $a = -0.25$, and $b = 0.5$. Two stable fixed points $x_{\mathbf{U}p} = 0.7071$ and $x_{\mathbf{D}own} = -0.7071$ are obtained using initial conditions (a) $x(0) = -3$ and (b) $x(0) = 3$.

strings, beam buckling, nonlinear electronic circuits, superconducting Josephson parametric amplifiers, ionization waves in plasma, and biological processes [Lakshmanan and Murali, 1996]. An interesting feature of this oscillator is the coexistence of two stable limit cycles for certain parameters.

It should be noted that synchronization and control of systems with coexisting attractors is not an easy task [Pisarchik et al., 2006; Pisarchik and Feudel, 2014]. Primary research of synchronization of bistable Duffing oscillators was limited to only two oscillators [Lakshmanan and Murali, 1996; Pisarchik and Jaimes-Reategui, 2005]. It was found that for a certain coupling strength these oscillators exhibit intermittent lag synchronization, when the coupling is unidirectional [Pisarchik and Jaimes-Reategui, 2005]. Notably, within time windows, when the two oscillators stay in the same state, anticipated synchronization occurs [Pisarchik et al., 2006; Sausedo-Solorio and Pisarchik, 2014].

In spite of extensive research on synchronization in coupled nonlinear oscillators [Boccaletti et al., 2018], not many papers are devoted to synchronization and control of multistable systems (see, e.g., [Pisarchik et al., 2006; Pisarchik and Feudel, 2014; Grubov et al., 2017; Jaimes-Reategui et al., 2017; Magallon-Garcia et al., 2017; Moskalenko et al., 2017] and references therein). Since the Duffing oscillator is the prototypical model which exhibits bistability, in this paper we use this oscillator to study self-organization in network motifs formed by bistable systems. For all possible configurations, we show how synchronization emerges as the coupling strength is increased, and how this system transforms from multistable to monostable.

The rest of the paper is organized as follows. In Sec. 2 we describe the model of the bistable Duffing oscillator. Then, in Section 3 we present and classify all possible network motifs and derive their equations of motion. Next, in Sections 4 and 5 we study synchronous dynamics of network motifs coupled in linear and ring configurations, respectively. Finally, in Section 6 we summarize the results.

2 Duffing Oscillator

The Duffing equation is given as

$$\frac{d^2x}{dt^2} + \gamma\frac{dx}{dt} + ax + bx^3 = f(t), \tag{1}$$

where $\gamma > 0$ and $f(t) = f\sin(\omega t)$. The variable x describes the motion of a particle of unit mass in the potential well

$$V(x) = \frac{1}{2}ax^2 + \frac{1}{4}bx^4 \tag{2}$$

under external periodic force $f(t)$ with period $T = 2\pi/\omega$ and strength f.

Depending on the relationship between parameters a and b, three types of the potential well can be distinguished.

(i) $a < 0$ and $b > 0$. A double-well potential with minima at $x = \pm\sqrt{\frac{|a|}{b}}$ and a local maximum at $x = 0$.

(ii) $a > 0$ and $b > 0$. A single-well potential with minima at equilibrium point $x = 0$.

(iii) $a > 0$ and $b < 0$. A double-hump potential well with a local minimum at $x = 0$ and maxima at $x = \pm\sqrt{\frac{|a|}{b}}$.

Each one of the above three cases has become a classical model to describe inherently nonlinear phenomenon, exhibiting a rich and baffling variety of regular (periodic) and complex (chaotic) motions which can coexist. In this

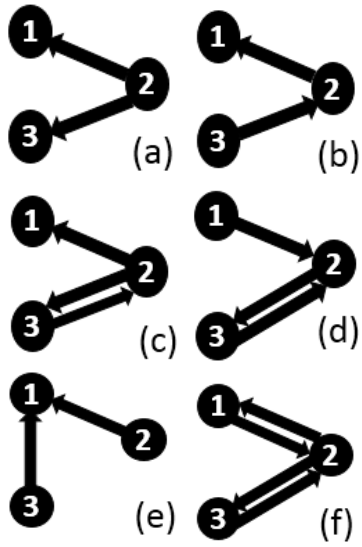

Figure 3. Network motifs in linear configuration representing (a) auxiliar, (b) chain, (c) mixed slave, (d) mixed master, (e) competitive, and (f) relay types of coupling schemes.

work we are interested in the first case shown in Fig. 1. This double-well potential Eq. (2) with $a = -0.25$ and $b = 0.5$ has minima at $x_{\mathbf{D}own} = -\sqrt{\dfrac{|a|}{b}} = -0.7$ and $x_{\mathbf{U}p} = \sqrt{\dfrac{|a|}{b}} = 0.7$ and a local maximum at $x = 0$.

The time series of Eq. (1) obtained using two different initial conditions are illustrated in Fig. 2. One can see that the asymptotic states are two equilibria at $x_{\mathbf{U}p} = 0.7071$ and $x_{\mathbf{D}own} = -0.7071$.

3 Network Motifs

Network motifs can be thought of as recurring circuits of interactions from which the networks are built [Alon, 2007]. Their presence indicates the operation of underlying nonrandom structural or evolutionary design principles that might have been involved in building the network [Stone et al., 2019].

In order to proceed, we define a few basic terms from the network theory [Boccaletti et al., 2006]. Any network or a graph may be studied in terms of its binary adjacency matrix $\mathbf{A}$. For a network with n nodes and an $n \times n$ binary adjacency matrix $\mathbf{A}$, $\mathbf{A}_{ij} = 1$ implies that the i-th node is connected to the j-th node and $\mathbf{A}_{ij} = 0$ otherwise. Undirected links impose no order on the nodes that they connect; the adjacency matrix for undirected networks is symmetric, i.e. $\mathbf{A}_{ij} = \mathbf{A}_{ji}$.

Network motifs formed by three coupled oscillators can be classified into 13 different configurations [Boccaletti et al., 2018] shown Figs. 3 and 4. The coupling can be either unidirectional, bidirectional, or combine.

Figures 3(a–f) represent network motifs formed by three oscillators coupled in a line. In particular, the auxiliar coupling scheme (Fig. 3(a)) consists in one master system (oscillator 2) and two slave systems (oscillators 1 and 3). Likewise, Fig. 3(b) shows the chain network motif, where oscillator 2 is a slave of oscillator 3 and at the same time a master of oscillator 1. Figures 3(c) and 3(d) illustrate network motifs with mixed coupling schemes. Here, oscillator 1 acts as either a slave (Fig. 3(c)) or a master (Fig. 3(d)) only. Meanwhile, the competitive coupling schemes is shown in Fig. 3(e), where oscillator 1 is a slave for both master oscillators 2 and 3. Finally, the mutual coupling configuration is shown in Fig. 3(f) which is also referred to as a relay coupling scheme.

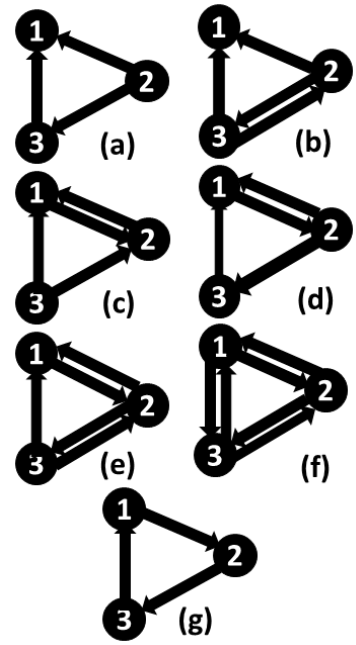

Figure 4. Network motifs in ring configuration representing (a) unidirectional auxiliar, (b) bidirectional competitive, (c) bidirectional auxiliar, (d) bidirectional mixed, (e) bidirectional double mixed, (f) bidirectional chain, and (g) unidirectional chain coupling schemes.

The ring coupling schemes are shown in Fig. 4. In the network motif shown in Fig. 4(a), all oscillators act simultaneously as a slave and a master. Instead, in the network motif in Fig. 4(b) oscillator 1 is only a slave, while other oscillators 2 and 3 are mutually coupled and act as a master for oscillator 1 and as both for themselves. Figure 4(c) shows the network motif where oscillator 3 is only a master for both oscillators 1 and 2 which are mutually coupled. The motif in Fig. 4(d) in similar to the motif in Fig. 4(a) with unidirectional coupling, but in another direction. In the motif in Fig. 4(e) all oscillators act as a slave and a master, but only oscillators 1 and 2 are mutually coupled. Similarly, in Figs. 4(f) and 4(g) all oscillators simultaneously act as a slave and a master,

Table 1. Equations of motion for linear network motifs

Network motif	Equation of motion
Fig. 3(a)	$\ddot{x}_1 = -\gamma\dot{x}_1 - ax_1 - bx_1^3 + \sigma(x_2 - x_1)$, $\ddot{x}_2 = -\gamma\dot{x}_2 - ax_2 - bx_2^3$, $\ddot{x}_3 = -\gamma\dot{x}_3 - ax_3 - bx_3^3 + \sigma(x_2 - x_3)$
Fig. 3(b)	$\ddot{x}_1 = -\gamma\dot{x}_1 - ax_1 - bx_1^3 + \sigma(x_2 - x_1)$, $\ddot{x}_2 = -\gamma\dot{x}_2 - ax_2 - bx_2^3 + \sigma(x_3 - x_2)$, $\ddot{x}_3 = -\gamma\dot{x}_3 - ax_3 - bx_3^3$
Fig. 3(c)	$\ddot{x}_1 = -\gamma\dot{x}_1 - ax_1 - bx_1^3 + \sigma(x_2 - x_1)$, $\ddot{x}_2 = -\gamma\dot{x}_2 - ax_2 - bx_2^3 + \sigma(x_3 - x_2)$, $\ddot{x}_3 = -\gamma\dot{x}_3 - ax_3 - bx_3^3 + \sigma(x_2 - x_3)$
Fig. 3(d)	$\ddot{x}_1 = -\gamma\dot{x}_1 - ax_1 - bx_1^3$, $\ddot{x}_2 = -\gamma\dot{x}_2 - ax_2 - bx_2^3$ $+\sigma(x_1 - x_2) + \sigma(x_3 - x_2)$, $\ddot{x}_3 = -\gamma\dot{x}_3 - ax_3 - bx_3^3 + \sigma(x_2 - x_3)$
Fig. 3(e)	$\ddot{x}_1 = -\gamma\dot{x}_1 - ax_1 - bx_1^3$ $+\sigma(x_2 - x_1) + \sigma(x_3 - x_1)$, $\ddot{x}_2 = -\gamma\dot{x}_2 - ax_2 - bx_2^3$, $\ddot{x}_3 = -\gamma\dot{x}_3 - ax_3 - bx_3^3$
Fig. 3(f)	$\ddot{x}_1 = -\gamma\dot{x}_1 - ax_1 - bx_1^3 + \sigma(x_2 - x_1)$, $\ddot{x}_2 = -\gamma\dot{x}_2 - ax_2 - bx_2^3$ $+\sigma(x_1 - x_2) + \sigma(x_3 - x_2)$, $\ddot{x}_3 = -\gamma\dot{x}_3 - ax_3 - bx_3^3 + \sigma(x_2 - x_3)$

but in Fig. 4(f) two oscillators (1 and 3) are unidirectionally coupled and in Fig. 4(g) all oscillators are mutually coupled.

In Tables 1 and 2 we present the equations of motion for linear and ring network motifs shown in Figs. 3 and 4, respectively.

4 Dynamics of Linear Motifs

For numerical simulations, the second-order equations of motion given in Tables 1 and 2 were converted into the first order equations using the change of variable $\dot{x} \to y$. In Fig. 5 we show the bifurcation diagrams of local maxima of x_1, x_2, and x_3 with respect to the coupling strength σ for six linear motifs using zero initial conditions for variables y ($y_1 = y_2 = y_3 = 0$) and different initial conditions CI-i ($i = 1, \ldots, 6$) for variables x_1, x_2, and x_3 presented in Table 3.

4.1 Bifurcation Diagrams of the Auxiliar Motif

For initial conditions CI-1, the local maxima of the state variable x_1 always takes the value of $x_1 = -0.7071$ for all coupling strengths (black dots in Fig. 5A-(i)). At the same time, the local maxima of the state variable x_2 for the same initial conditions are equal (black dots in Fig. 5A-(ii)). By contrast, the local maxima of the state variable x_3 (black dots in Fig. 5 A-(iii)) take the value of $x_3 = 0.7071$. One can see from Fig. 5 A-(iii) that the local maxima first begin slowly decreasing as the coupling strength σ is increased up to $\sigma_{th} = 0.06$ and then switch to $x_3 = -0.7071$. This result can be explained by the fact that the auxiliar motif shown in Fig. 3 (a) is composed by one master (oscillator 2) and two slave systems (oscillators 1 and 3). Therefore, regardless initial conditions the slave oscillators driven by the master are attracted to the master's attractor when the coupling strength σ is increased and reaches a threshold value of $\sigma_{th} = 0.06$.

The bifurcation diagrams of the same motif for other initial conditions from Table 3 are shown in Fig. 3(a) by other colors, in particular, for the initial conditions CI-2 (blue dots), CI-3 (red dots), CI-4 (green dots), CI-5 (yellow dots), and CI-6 (purple dots). One can in Figs. 5A (i)–(iii) that the master system (oscillator 2) either stays in one the coexisting attractors $x_{down} = -0.7071$ or $x_{up} = 0.7$ (see Fig. 1) or the slave oscillators (oscillators 1 and 3) stay in the master's attractor when the coupling strength σ reaches the threshold value of $\sigma_{th} = 0.06$.

4.2 Bifurcation Diagrams of the Chain Motif

Figures 5B (i)–(iii) show the bifurcation diagrams for the chain network motif illustrated in Fig. 3(b). Starting from initial conditions CI-1 (see Table 3) $x_1(0) = x_2(0) = -0.7071$ and $x_3(0) = 0.7071$, the variables x_1 and x_2 slowly change as the coupling strength is increased up to $\sigma_{th} = 0.06$ and for higher values of σ these variables suddenly switch to $x_1 = x_2 = 0.7071$ (black dots in Fig. 5B (i)–(ii)), while x_3 remains the same (black dots in Fig. 5B (iii)). This result is expected since both oscillators 1 and 2 are slaves and driven by the oscillator 3. The driving first affects the oscillator 2 because it is a slave of the oscillator 3. In Fig. 5B (i) black dots show how the process is realized, namely, x_2 changes from $x_2 = -0.7071$ to $x_2 = -0.42$ as σ approaches $\sigma_{th} = 0.06$. As σ is further increased, the oscillator 3 drives the oscillator 1 thought the oscillator 2 because the oscillator 1 is a slave of the oscillator 2. This situation is illustrated in Fig. 5B (ii) by black dots which show the change of x_1 from $x_1 = -0.7071$ to $x_1 = -0.67$ as σ approaches $\sigma_{th} = 0.06$. For $\sigma > 0.06$ the both variables x_2 and x_1 are driven by the oscillator 3, that leads to their sudden switch to $x_1 = x_2 = x_3 = 0.7071$.

4.3 Bifurcation Diagrams of the Mixed Master Motif

Figures 5C (i)–(iii) show the bifurcation diagrams of the mixed master motif presented in Fig. 3(c). In this

Table 2. Equations of motion for ring network motifs

Network motif	Equation of motion
Fig.4(a)	$\ddot{x}_1 = -\gamma\dot{x}_1 - ax_1 - bx_1^3 + \sigma(x_2 - x_1) + \sigma(x_3 - x_1)$, $\ddot{x}_2 = -\gamma\dot{x}_2 - ax_2 - bx_2^3$, $\ddot{x}_3 = -\gamma\dot{x}_3 - ax_3 - bx_3^3 + \sigma(x_2 - x_3)$
Fig.4(b)	$\ddot{x}_1 = -\gamma\dot{x}_1 - ax_1 - bx_1^3 + \sigma(x_2 - x_1) + \sigma(x_3 - x_1)$, $\ddot{x}_2 = -\gamma\dot{x}_2 - ax_2 - bx_2^3 + \sigma(x_3 - x_2)$, $\ddot{x}_3 = -\gamma\dot{x}_3 - ax_3 - bx_3^3 + \sigma(x_2 - x_3)$
Fig.4(c)	$\ddot{x}_1 = -\gamma\dot{x}_1 - ax_1 - bx_1^3 + \sigma(x_2 - x_1) + \sigma(x_3 - x_1)$, $\ddot{x}_2 = -\gamma\dot{x}_2 - ax_2 - bx_2^3 + \sigma(x_2 - x_2) + \sigma(x_1 - x_2)$, $\ddot{x}_3 = \gamma\dot{x}_3 - ax_3 - bx_3^3$
Fig.4(d)	$\ddot{x}_1 = -\gamma\dot{x}_1 - ax_1 - bx_1^3 + \sigma(x_2 - x_1) + \sigma(x_3 - x_1)$, $\ddot{x}_2 = -\gamma\dot{x}_2 - ax_2 - bx_2^3 + \sigma(x_1 - x_2) + \sigma(x_3 - x_2)$, $\ddot{x}_3 = -\gamma\dot{x}_3 - ax_3 - bx_3^3 + \sigma(x_1 - x_3) + \sigma(x_2 - x_3)$
Fig.4(e)	$\ddot{x}_1 = -\gamma\dot{x}_1 - ax_1 - bx_1^3 + \sigma(x_2 - x_1) + \sigma(x_3 - x_1)$, $\ddot{x}_2\gamma\dot{x}_2 - ax_2 - bx_2^3 + \sigma(x_1 - x_2)$, $\ddot{x}_3 = -\gamma\dot{x}_3 - ax_3 - bx_3^3 + \sigma(x_2 - x_3)$
Fig.4(f)	$\ddot{x}_1 = -\gamma\dot{x}_1 - ax_1 - bx_1^3 + \sigma(x_2 - x_1) + \sigma(x_3 - x_1)$, $\ddot{x}_2 = -\gamma\dot{x}_2 - ax_2 - bx_2^3 + \sigma(x_1 - x_2) + \sigma(x_3 - x_2)$, $\ddot{x}_3 = -\gamma\dot{x}_3 - ax_3 - bx_3^3 + \sigma(x_2 - x_3)$
Fig.4(g)	$\ddot{x}_1 = -\gamma\dot{x}_1 - ax_1 - bx_1^3 + \sigma(x_3 - x_1)$, $\ddot{x}_2 = -\gamma\dot{x}_2 - ax_2 - bx_2^3 + \sigma(x_1 - x_2)$, $\ddot{x}_3 = -\gamma\dot{x}_3 - ax_3 - bx_3^3 + \sigma(x_2 - x_3)$

Table 3. Initial conditions CI-i ($i = 1, \ldots, 6$) used for simulations of equations of motion presented in Table 1.

CI$-i$	$x_1(0)$	$x_2(0)$	$x_3(0)$
CI-1	-0.7071	-0.7071	0.7071
CI-2	-0.7071	0.7071	-0.7071
CI-3	-0.7071	0.7071	0.7071
CI-4	0.7071	-0.7071	-0.7071
CI-5	0.7071	-0.7071	0.7071
CI-6	0.7071	0.7071	-0.7071

motif the oscillator 1 acts as a slave only, but the oscillators 2 and 3 are mutually coupled. The bifurcation diagrams in Fig. 5C (i) are constructed for CI-1 (black dots), CI-6 (purple dots), CI-2 (blue dots), and CI-5 (yellow dots) initial conditions, i.e., the initial conditions for the variables x_2 and x_3 have different signs, i.e. $x_2(0) = -0.7071$ and $x_3(0) = 0.7071$ or in reverse, while the variable x_1 starts either from $x_1(0) = -0.7071$ or $x_1(0) = 0.7071$. For example, for initial conditions CI-1 (black point in Fig. 5C (i)) with $x_1(0) = -0.7071$, $x_2(0) = -0.7071$, and $x_3(0) = 0.7071$ the local maxima of x_1 grow from negative to positive values, as the coupling strength σ is increased and reaches $\sigma = 0.17$. A further increase in σ results in decreasing x_1 up to zero for $\sigma_{th} = 0.25$, and then x_1 remains zero, as σ is further increased. An inverse behavior is observed for initial conditions CI-6 (purple dots), when the local maxima of x_1 decreases from positive to negative values, as σ is increased and reaches $\sigma = 0.17$. A further increase in σ results in increasing x_1 up to zero, i.e., $x_1 = 0$ for $\sigma_{th} = 0.25$ and remains constant as σ is increased. We should note that the transition of x_1 from either $x_1(0) = -0.7071$ or $x_1(0) = -0.7071$ to a new fixed point $x_1 = 0$ needs a higher value of $\sigma_{th} = 0.25$, i.e., the system is more resistant to a change in the coupling strength.

On the other hand, one can see in Fig. 5C (i) that the bifurcation diagrams CI-2 (blue dots) and CI-5 (yellow dots) behave the same as the bifurcation diagrams CI-2 (black dots) and CI-5 (purple dots), respectively, but with the difference that the transition of x_1 from either $x_1(0) = 0.7071$ or $x_1(0) = -0.7071$ to the new fixed point $x_1 = 0$ does not pass through zero. Also, x_1 approaches $x_1 = 0$ for a weaker coupling ($\sigma_{th} = 0.13$) because the initial condition for x_2 has opposite sign than for x_1 and x_3. Likewise, as x_2 acts as a master for the oscillators 1, the oscillator x_3 acts as both a master and a slave. As σ is increased, a strong competition between x_2 and x_3 arises, since initially they had opposite signs and consequently x_1 goes faster to the fixed point $x_1 = 0$.

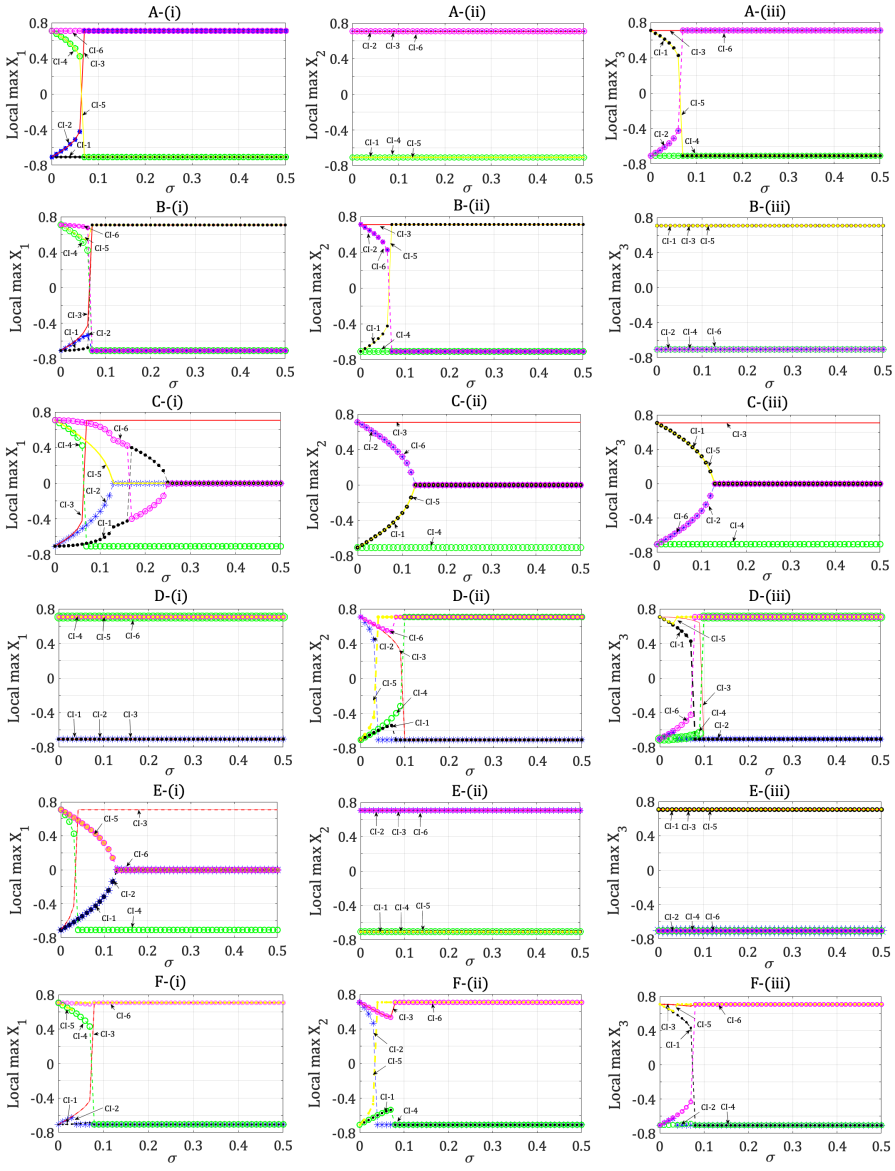

Figure 5. Bifurcation diagrams of local maxima using coupling strength σ as a control parameter for linear network motifs presented in Fig. 3. Coexisting attractors are shown by different colors.

The last results can be explained as follows. The Duffing oscillator with parameters used in this work has an unstable fixed point $x = 0$ and two stable fixed points $x_{down} = -0.7071$ and $x_{up} = 0.7071$ (see Fig. 1), which we take as initial conditions $x_1(0) = -0.7071$ and $x_1(0) = 0.7071$. Likewise, in Fig. 5 C (i) x_1 starting from any of the stable fixed points x_{down} or x_{up} approaches the new stable fixed point $x_1 = 0$ as the coupling strength σ is increased and reaches σ_{th}. Such a behavior results from the fact that the oscillators 2 and 3 are mutually coupled and have initial conditions of opposite signs. Therefore, there is a strong competition between them. When σ approaches σ_{th}, both x_2 and x_3 tend toward the same new fixed point $x_2 = x_3 = 0$. Moreover, as the oscillator 1 is a slave only and it is driven by the oscillator 2, x_1 changes to the new fixed point $x_1 = 0$. In addition, the oscillators 1, 2, and 3 being uncoupled have unstable fixed point $x = 0$, whereas when they are coupled in the network motif shown in Fig. 3(c) and the coupling strength reaches the threshold value σ_{th}, this unstable fixed point $x = 0$ becomes stable.

By contrast, for the initial conditions corresponding to CI-3 (red dots) and CI-4 (green dots), the bifurcations diagrams of x_1 shown in Fig. 5C (i)–(iii) have a completely different behaviour than for the initial conditions CI-1 (black dots), CI-6 (purple dots), CI-2 (blue dots), and CI-5 (yellow dots). Since the oscillators 2 and 3 are mutually coupled and their initial conditions have the same sign, they do not change, i.e. $x_2 = x_3 = 0.7071$ or $x_2 = x_3 = -0.7071$ as the coupling strength σ is increased. At the same time, since the oscillator 1 is a slave only, x_1 is driven by the oscillators 2 and 3 and as a result

it changes to $x_1 = 0.7071$ or $x_1 = -0.7071$ when its initial conditions are $x_1(0) = -0.7071$ or $x_1(0) = 0.7071$, respectively.

As can be observed in the bifurcation diagrams shown in Figs. 5C (ii) and (iii), x_2 and x_3 behave similarly. In particular, the bifurcation diagram CI-1 (black dots), CI-6 (purple dots), CI-2 (blue dots), and CI-5 (yellow dots) correspond to the mutually coupled oscillators 2 and 3 with initial conditions of opposite sign, and therefore there is a strong competition between them as σ is increased approaching $\sigma_{th} = 0.13$ where the both state variables x_2 and x_3 tend toward the same new fixed point $x_2 = x_3 = 0$ (see Figs. 5C (ii) and (iii)). At the same time, in the bifurcation diagrams CI-3 (red dots) and CI-4 (green circle) x_2 and x_3 with initial conditions of the same sign remain the same, either $x_2 = x_3 = 0.7$ or $x_2 = x_3 = -0.7$ as σ is increased (see Figs. 5C (ii) and (iii)).

4.4 Bifurcation Diagrams of the Mixed Slave Motif

In Figs. 5D (i)–(iii) we plot the bifurcation diagrams of the local maxima of the state variable x_1, x_2, and x_3 of the oscillators 1, 2, and 3, respectively, corresponding to the mixed slave network motif presented in Fig. 3(d) and their evolution equations shown in Table 1. These diagrams start from $x_1(0) = x_2(0) = -0.7071$ and $x_3(0) = 0.7071$ corresponding to the initial condition CI-1 (see Table 3). Since the oscillators 2 and 3 are mutually coupled, they act as both a master and a slave. However, for $\sigma > 0.07$ these state variables x_2 and x_3 are driven by the oscillators 1 and change their values to $x_1 = x_2 = x_3 = -0.7071$ (black dots). A similar behaviour is observed in the remaining bifurcation diagrams CI-2 (blue dots) for $\sigma_{th} = 0.03$, CI-3 (red dots) for $\sigma_{th} = 0.09$, CI-4 (green dots) for $\sigma_{th} = 0.09$, CI-5 (yellow dots) for $\sigma_{th} = 0.03$, and CI-6 (purple dots) for $\sigma_{th} = 0.07$ in Figs. 5D (i)– (iii), where again the oscillator 1 is a master only and the oscillators 2 and 3 are mutually coupled. As a result, the state variable x_2 and x_3 adjust their behavior to each other when $\sigma < \sigma_{th}$, and for $\sigma > \sigma_{th}$ they change their value to $x_2 = x_3 = x_1 = -0.7071$ because of the driving by the oscillator 1. The value of the threshold coupling strength σ_{th} depends on the initial conditions (see Table 3).

4.5 Bifurcation Diagrams of the Competitive Motif

The bifurcation diagrams in Figs. 5E (i)–(iii) show the local maxima of x_1, x_2, and x_3 for the competitive network motif illustrated in Fig. 3(e). Their evolution equations are present in Table 1. The bifurcation diagrams in Figs. 5E (i) and 5C (i) have similar behaviours, they possess a strong dependence on initial conditions. Since the oscillators 2 and 3 are only masters for the oscillators 1 and their initial conditions have opposite signs $x_1(0) = -0.7071$ or $x_1(0) = 0.7071$ (CI-1 – CI-6 and CI-2 – CI-5 in Table 3), there is a strong competition with the oscillator 1 as σ is increased. When σ approches σ_{th} the oscillator 1 tends toward a new fixed point $x_1 = 0$ due to the driving by the oscillators 2 and 3 (see the bifurcation diagrams CI-1 (black dots) – CI-6 (purple dots) and CI-2 (blue dots) – CI-5 (yellow dots) in Fig. 5E (i)). One can see that the bifurcation diagrams constructed for the initial conditions CI-3 and CI-4 (see Table 3) differ from the diagram for the initial conditions described above. The master oscillators 2 and 3 starting from the same initial condition ($x_2 = x_3 = 0.7071$ or $x_2 = x_3 = -0.7071$) conserve this value as σ is increased, whereas the slave oscillator 1 changes to $x_1 = 0.7071$ or $x_1 = -0.7071$ depending on the initial condition either $x_1(0) = -0.7071$ or $x_1 = 0.7071$ (CI-3 (red dots) and CI-4 (green dots)).

In the bifurcation diagrams in Figs. 5E (ii)–(iii), x_2 and x_3 also conserve their values as σ is increased, because the both oscillators are masters for the oscillators 1 and start from the same initial conditions (see Table 3), i.e. $x_2 = x_3 = 0.7071$ or $x_2 = x_3 = -0.7071$ (CI-1 (black dots), CI-2 (blue dots), CI-3 (red dots), CI-4 (green dots), CI-5 (yellow dots) and CI-6 (purple dots)).

4.6 Bifurcation Diagrams of the Relay Motif

The bifurcation diagrams for the relay network motif presented in Fig. 3(f) are shown in Figs. 5F (i)–(iii). When two state variables x_1 and x_3 start from the same initial conditions (see Table 3, they conserve their values as σ is increases, whereas x_2 starting from different initial condition is driven by the oscillators 1 and 3 up to $\sigma = \sigma_{th}$ which depends on the initial conditions. In particular, starting from $x_1(0) = x_2(0) = -0.7071$ and $x_3(0) = 0.7071$ (initial condition CI-1) both x_1 and x_2 increase as the coupling strength grows up to $\sigma_{th} = 0.03$ for x_1 and $\sigma_{th} = 0.07$ for x_2, and then with a further increase in σ they return again to $x_1 = x_2 = -0.7$ and conserve this value (black dots in Figs. 5F (i) and (ii), respectively). However, the state variables x_3 starting from $x_3(0) = 0.7071$ first decreases as σ is increased and reaches $\sigma_{th} = 0.07$ and then for $\sigma > 0.07$ this variable approaches $x_3 = -0.7071$ as σ is further increased. A similar behaviour is also observed in other bifurcation diagrams constrained for CI-2 (blue dots), CI-3 (red dots), CI-4 (green dots), CI-5 (yellow dots), and CI-6 (purple dots) in Figs. 5F (i)–(iii).

5 Dynamics of Ring Motifs

In Fig. 6 we plot the bifurcation diagrams of the local maxima of the variables x_1, x_2, and x_3 for seven ring configurations of the networks motifs presented in Fig. 4, as a function of the couple strength σ for six different initial conditions CI-i $i = 1, \ldots, 6$ (see Table 3).

Looking at the bifurcation diagrams for the ring motifs, one can notice that the dynamics of the motifs presented in Figs. 4(a,c,f) are more poor than others. These configurations belong to unidirectional auxiliar, bidirectional auxiliar, and bidirectional chain coupling schemes. For these motifs, the whole system exhibits the

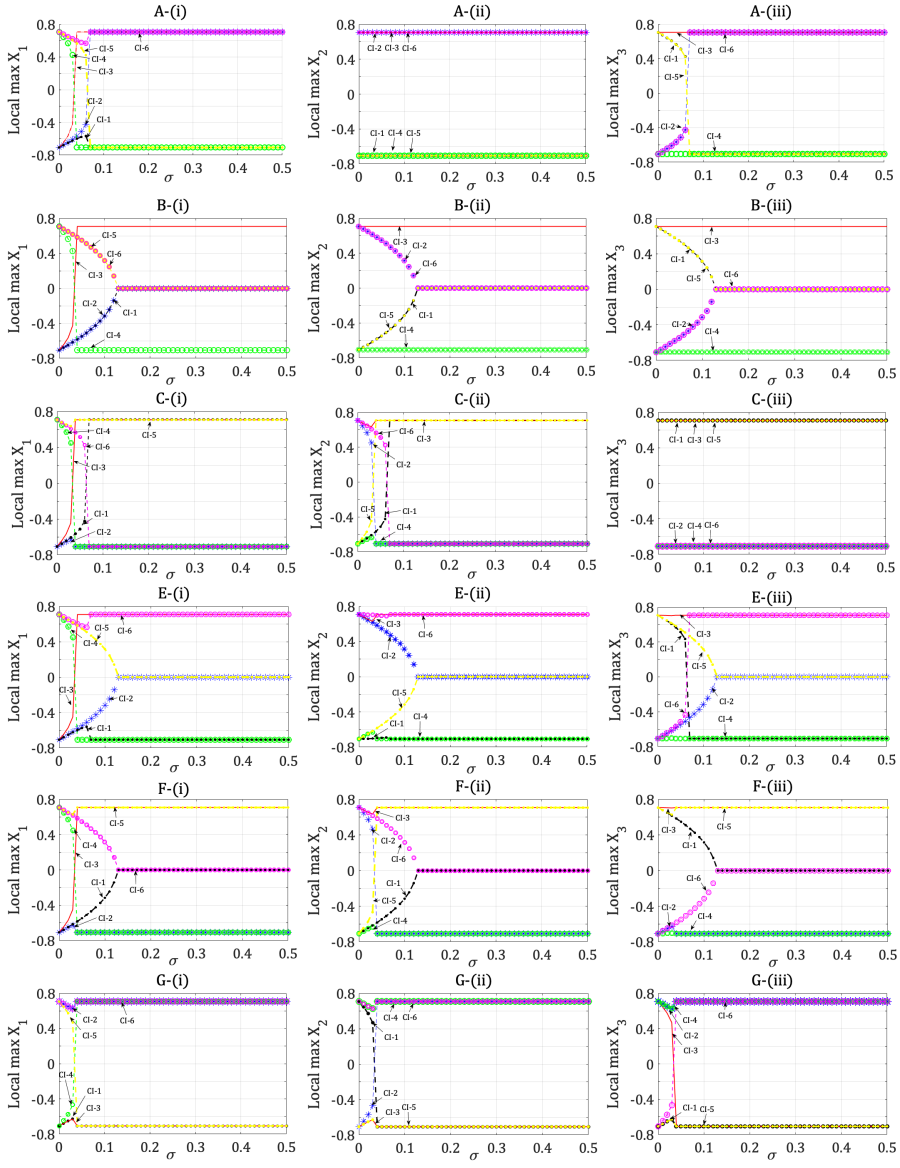

Figure 6. Bifurcation diagrams of local maxima using coupling strength σ as a control parameter for ring network motifs presented in Figs. 4(a–f). Coexisting attractors found using different initial conditions are shown by different colors: CI-(black dots), CI-2 (blue dots), CI-3 (red dots), CI-4 (green dots), CI-5 (yellow dots), and CI-6 (purple dots).

coexistence of only two stable fixed point for $\sigma > 0.05$. A single limit cycle exists only for very small coupling ($\sigma < 0.05$). This can be explained by the fact that in these configurations all oscillators act as one, even when the coupling is not very strong.

Instead, the motifs presented in Figs. 4(b,d,e) (bidirectional competitive, bidirectional mixed, and bidirectional double mixed) display very rich dynamics due to a strong competition between the oscillators. For these schemes we observe the coexistence of three attractors. For relatively small coupling ($\sigma < 0.15$) two fixed points coexist with a limit cycle, whereas for stronger coupling the limit cycle converts into a zero steady state in the Hopf bifurcation.

The most complex dynamics is observed for the unidirectional chain motif presented in Fig. 4(g). Its bifurcation diagrams are shown in Figs. 7 (i)–(iii) for different initial conditions CI-(black dots), CI-2 (blue dots), CI-3 (red dots), CI-4. In this motif, each oscillator acts simultaneously as a master and as a slave. Likewise, regardless a sign of the initial conditions there are two Hopf bifurcation points where the oscillators begin oscillate with the same frequency (at $\sigma = 0.36$) and then another frequency appears (at $\sigma = 0.48$), as the coupling strength is increased.

These results confirm previous observations on the route to quasiperiodicity in ring motifs of discrete systems formed by logistic [Pisarchik et al., 2019] and Rulkov maps [Sausedo-Solorio and Pisarchik, 2017].

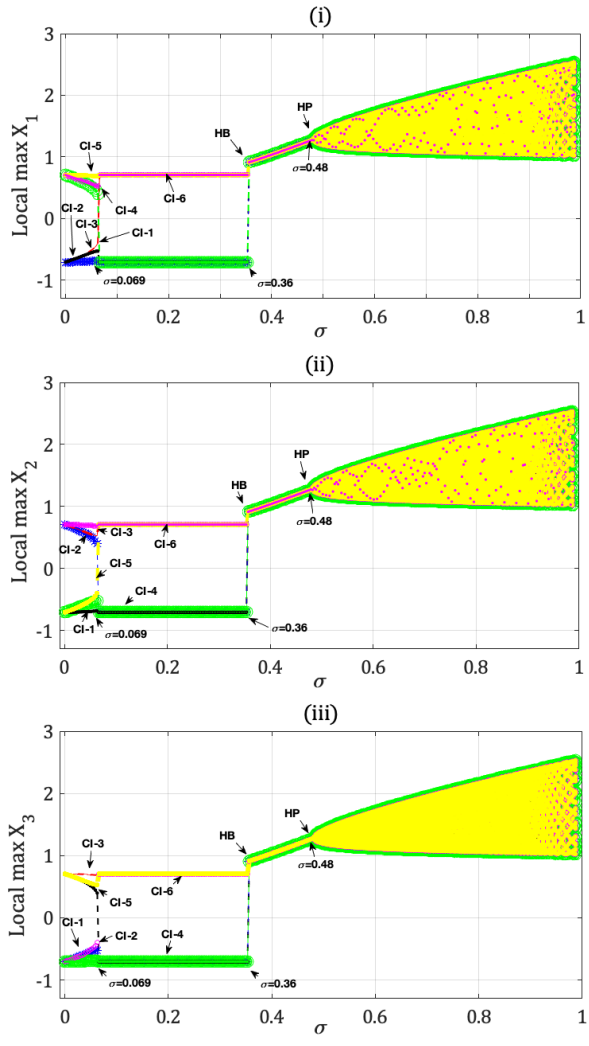

Figure 7. Bifurcation diagrams of local maxima using coupling strength σ as a control parameter for the unidirectionally chain motif presented in Fig. 4(g). The colors correspond to the same initial conditions as in Fig. 6. HB and HP are Hopf bifurcations where a periodic and a quasiperiodic orbits are born.

6 Conclusion

We have studied dynamics of network motifs formed by three Duffing oscillators coupled in different configurations. The bifurcation analysis have shown that depending on the coupling strength and configuration, these motifs can exhibit either monostability, bistability, or multistability. We have demonstrated different scenarios from bistability to monostability with respect to the coupling strength for all possible configurations.

The richest dynamics is observed in the unidirectionally chain motif. Apart from bistability, this configuration allows transitions to periodicity and quasiperiodicity, as the coupling strength is increased.

We believe that the obtained results have a general character for this class of systems, since similar dynamics has been found in other ring-coupled oscillators [Pisarchik et al., 2019; Sausedo-Solorio and Pisarchik, 2017].

Acknowledgements

The numerical simulations and analysis were supported by the project "Equipamientos de los laboratorios de investigacion de los cuerpos academicos de CULAGOS con orientación optoelectronica, R-0138/2016, Agreement RG /019/2016-UdeG, and RC/075/2018, AgreementRG/006/2018, UDG. A.N.P. acknowledges support from the Russian Science Foundation (Grant No. 19-12-00050) for the main concept of this work.

References

Andrievskii, B. R. and Fradkov, A. L. (2004). Control of chaos: Methods and applications. II: Applications. *Automation and Remote Control* **65**(4), 505–533.

Alon, U. (2007). Network motifs: Theory and experimental approaches. *Nat. Rev. Genetics* **8**(6), 450–461.

Boccaletti, S. and Latora, V., Moreno, Y., Chavez, M., and Hwang, D. U. (2006). Complex networks: Structure and dynamics. *Phys. Rep.* **424**(4–5), 175–308.

Boccaletti, S., Pisarchik, A. N., del Genio, C. I., and Amann, A. (2018). *Synchronization: From Coupled Systems to Complex Networks* (Cambridge University Press).

Duffing, G. (1918). Erzwungene Schwingungen bei veränderlicher Eigenfrequenz und ihre technische Bedeutung, No. 41–42 (F. Vieweg – sohn.).

Jaimes-Reátegui, R., García-Vellisca, M. A., Pisarchik, A. N., and del Pozo-Guerrero, F. (2017). Bistability in Hindmarsh-Rose oscillators induced by asymmetric electrical coupling. *Cybernetics and Physics* **6**, 126-–130.

Jaros, P., Kapitaniak, T. and Perlikowski, P. (2016). Multistability in nonlinearly coupled ring of Duffing systems. *Eur. Phys. J. Spec. Top.* **225** (13–14), 2623–2634.

Grubov, V., Runnova, A., Zhuravlev, M., Maksimenko, V., Pchelintseva, S., and Pisarchik, A. (2017). Perception of multistable images: EEG studies. *Cybernetics and Physics* **6**, 103—107.

Jaros, P., Perlikowski, P., and Kapitaniak, T. (2015). Synchronization and multistability in the ring of modified Rössler oscillators. *Eur. Phys. J. Spec. Top.* **224**(8), 1541–1552.

Karakaya, B., Minati, L., Gambuzza, L. V., and Frasca, M. (2019). Fading of remote synchronization in tree networks of Stuart-Landau oscillators. *Phys. Rev. E* **99**, 052301.

Lakshmanan, M. and Murali, K. (1996). *Chaos in Nonlinear Oscillators: Controlling and Synchronization* **13** (World Scientific).

Magallón-García, D. A., Jaimes-Reátegui, R., Huerta-Cuellar, G., Gallegos-Infante, L. A., Soria-Fregoso, C., and García-López, J. H. (2017). Study of multistable visual perception using a synergetic model. *Cybernetics and Physics* **6**, 120-–126.

Milo, R., Shen-Orr, S., Itzkovitz, S., Kashtan, N., Chklovskii, D., and Alon, U. (2002). Network motifs: simple building blocks of complex networks. *Science* **298**(5594), 824–827.

Mirasso, C. R., Carelli, P. V., Pereira, T., Matias, F. S., and Copelli, M. (2017). Anticipated and zero-lag synchronization in motifs of delay-coupled systems, *Chaos* **27**, 114305.

Moskalenko, O. I., Koronovskii, A., Hramov, A. E., Zhuravlev, M. O., and Jaimes-Reátegui, R. (2017). Residence time distributions for coexisting regimes of bistable dynamical systems subjected to noise influence. *Cybernetics and Physics* **6**, 97—102.

Pisarchik, A. N. and Feudel, U. (2014). Control of multistability. *Phys. Rep.* **54**, 167–218.

Pisarchik, A. N. and Jaimes-Reategui, R. (2005). Intermittent lag synchronization in a nonautonomous system of coupled oscillators. *Phys. Lett. A* **338**(2), 141–149.

Pisarchik, A. N., Jaimes-Reátegui, R., Villalobos-Salazar, J. R., Garcia-Lopez, J. H., and Boccaletti, S. (2006). Synchronization of chaotic systems with coexisting attractors. *Phys. Rev. Lett.* **96**(24), 244102.

Pisarchik, A. N., Bashkirtseva, I. A., and Ryashko, L. B. (2019). Noise-induced quasiperiodicity in a ring of unidirectionally-coupled nonidentical maps. *Phys. Lett. A* **383**, 1571–1577.

Sausedo-Solorio, J. M. and Pisarchik, A. N. (2014). Synchronization of map-based neurons with memory and synaptic delay. *Phys. Lett. A* **378**, 2108–2112.

Sausedo-Solorio, J. M. and Pisarchik, A. N. (2017). Synchronization in network motifs of delay-coupled map-based neurons. *Eur. Phys. J. Spec. Top.* **226**(9), 1911–1920.

Stone, L., Simberloff, D., and Artzy-Randrup, Y. (2019). Network motifs and their origins. *PLoS Comput. Biol.* **15**(4), 2623–2634.

Suresh, R., Senthilkumar, D. V., Lakshmanan, M., and Kurths, J. (2016). Emergence of a common generalized synchronization manifold in network motifs of structurally different time-delay systems. *Chaos Soliton Fract. 93*, 235–245.